WAPD-TM-1307

DEPARTMENT OF ENERGY RESEARCH
AND DEVELOPMENT REPORT

MONTE CARLO ANALYSES OF TRX SLIGHTLY ENRICHED URANIUM-H_2O CRITICAL EXPERIMENTS WITH ENDF/B-IV AND RELATED DATA SETS

(AWBA DEVELOPMENT PROGRAM)

DECEMBER 1977

CONTRACT EY-76-C-11-0014

BETTIS ATOMIC POWER LABORATORY
WEST MIFFLIN, PENNSYLVANIA

Operated for the U. S. Department of Energy by
WESTINGHOUSE ELECTRIC CORPORATION

DISCLAIMER

WAPD-TM-1307

MONTE CARLO ANALYSES OF TRX SLIGHTLY ENRICHED URANIUM-H_2O CRITICAL EXPERIMENTS WITH ENDF/B-IV AND RELATED DATA SETS

(AWBA DEVELOPMENT PROGRAM)

J. Hardy, Jr.

CONTRACT NO. EY-76-C-11-0014

DECEMBER 1977

Printed in the United States of America
Available from the
National Technical Information Service
U. S. Department of Commerce
5285 Port Royal Road
Springfield, Virginia 22151

NOTE

This document is an interim memorandum prepared primarily for internal reference and does not represent a final expression of the opinion of Westinghouse. When this memorandum is distributed externally, it is with the express understanding that Westinghouse makes no representation as to completeness, accuracy, or usability of information contained therein.

BETTIS ATOMIC POWER LABORATORY WEST MIFFLIN, PENNSYLVANIA

Operated for the U. S. Department of Energy by
WESTINGHOUSE ELECTRIC CORPORATION

NOTICE

FOREWORD

The Shippingport Atomic Power Station located in Shippingport, Pennsylvania was the first large-scale, central-station nuclear power plant in the United States and the first plant of such size in the world operated solely to produce electric power. This project was started in 1953 to confirm the practical application of nuclear power for large-scale electric power generation. It has provided much of the technology being used for design and operation of the commercial, central-station nuclear power plants now in use.

Subsequent to development and successful operation of the Pressurized Water Reactor in the AEC-owned reactor plant at the Shippingport Atomic Power Station, the Atomic Energy Commission in 1965 undertook a research and development program to design and build a Light Water Breeder Reactor core for operation in the Shippingport Station. In 1976, with fabrication of the Light Water Breeder Reactor (LWBR) nearing completion the Energy Research and Development Administration established the Advanced Water Breeder Applications program (AWBA) to develop and disseminate technical information which would assist U.S. industry in evaluating the LWBR concept. All three of these reactor development projects have been administered by the Division of Naval Reactors with the goal of developing practical improvements in the utilization of nuclear fuel resources for generation of electrical energy using water-cooled nuclear reactors.

The objective of the Light Water Breeder Reactor project has been to develop a technology that would significantly improve the utilization of the nation's nuclear fuel resources employing the well-established water reactor technology. To achieve this objective, work has been directed toward analysis, design, component tests, and fabrication of a water-cooled, thorium oxide fuel cycle breeder reactor to install and operate at the Shippingport Station. Operation of the LWBR core in the Shippingport Station started in the Fall of 1977 and is expected to be completed in about 3 to 4 years. Then the fissionable fuel inventory of the core will be measured. This effort, when completed in about 2 to 3 years after completion of LWBR core operation, is expected to confirm that breeding actually took place.

The Advanced Water Breeder Applications (AWBA) project was initiated to develop and disseminate technical information that will assist U.S. industry in evaluating the LWBR concept for commercial-scale applications. The project will explore some of the problems that would be faced by industry in adapting technology confirmed in the LWBR program. Information to be developed includes concepts for commercial-scale prebreeder cores which will produce uranium-233 for light water breeder cores while producing electric power, improvements for breeder cores based on the technology developed to fabricate and operate the Shippingport LWBR core, and other information and technology to aid in evaluating commercial-scale application of the LWBR concept.

Technical information developed under the Shippingport, LWBR, and AWBA projects has been and will continue to be published in technical memoranda, one of which is this present report.

CONTENTS

LIST OF FIGURES

ABSTRACT

Four H_2O-moderated, slightly-enriched-uranium critical experiments were analyzed by Monte Carlo methods with ENDF/B-IV data. These were simple metal-rod lattices comprising Cross Section Evaluation Working Group thermal reactor benchmarks TRX-1 through TRX-4. Generally good agreement with experiment was obtained for calculated integral parameters: the epi-thermal/thermal ratio of U238 capture (ρ^{28}) and of U235 fission (δ^{25}), the ratio of U238 capture to U235 fission (CR*), and the ratio of U238 fission to U235 fission (δ^{28}). Full-core Monte Carlo calculations for two lattices showed good agreement with cell Monte Carlo-plus-multigroup P_ℓ leakage corrections. Newly measured parameters for the low energy resonances of U238 significantly improved ρ^{28}. In comparison with other CSEWG analyses, the strong correlation between K_{eff} and ρ^{28} suggests that U238 resonance capture is the major problem encountered in analyzing these lattices.

MONTE CARLO ANALYSES OF TRX SLIGHTLY ENRICHED URANIUM-H_2O CRITICAL EXPERIMENTS WITH ENDF/B-IV AND RELATED DATA SETS

(AWBA Development Program)

J. Hardy, Jr.

I. INTRODUCTION

Four H_2O-moderated, slightly-enriched-uranium critical experiments have been analyzed with ENDF/B-IV data in connection with the data testing effort of the Cross Section Evaluation Working Group (CSEWG). These experiments were simple metal-rod lattices (Ref. 1) comprising CSEWG thermal reactor benchmarks TRX-1 through TRX-4 (Ref. 2). The purpose of this analysis is to obtain a clean test of the ability of ENDF/B-IV data to predict the neutron economy in lattices of this type.

The fuel rods were of uranium (enriched to 1.3% U235) clad in aluminum. They were 48 inches long and of 0.387 inch diameter, arranged in hexagonal arrays at water/fuel volume ratios of 2.35, 4.02, 1.00, and 8.11. TRX-1 and 2 were full lattices; TRX-3 and 4 were run as inner lattices surrounded by driver regions of high-density UO_2 rods. All lattices were fully reflected and their perimeters were made as nearly circular as possible. They were operated at room temperature.

The following parameters were measured at the center of each lattice: the epi-thermal/thermal ratio of U238 capture (ρ^{28}) and of U235 fission (δ^{25}), the ratio of U238 capture to U235 fission (CR*), and the ratio of U238 fission to U235 fission (δ^{28}). At core center, the flux spectra were asymptotic in the full lattices; they were not quite asymptotic in the two-region lattices (TRX-3 and TRX-4). Axial and radial bucklings were measured in the full lattices.

The parameters have been calculated by a method which has been used for several years. First, a full-energy-range cell calculation (zero leakage) was done with the RCP01 Monte Carlo program, an expanded version of RECAP (Ref. 3). Relatively small leakage corrections to the cell reaction rates were then obtained from a full-core analysis with the multigroup P_ℓ program P7MG, an extension of P3MG (Ref. 4), which treated a homogenized lattice. Intracell flux weighting factors in P7MG were chosen to match Monte Carlo reaction rates in the zero-leakage cell.

Calculated parameters obtained in this manner with ENDF/B-IV data are compared with measured values and with corresponding results from earlier ENDF versions. Results are also presented for cross section variations potentially affecting U238 capture. These include new resonance parameter values for the low-energy U238 resonances and two changes of U238 resonance cross section representation which affect the σ_s profile: inclusion of negative energy resonances and use of a multilevel description. Several variations of the U235 fission spectrum, which primarily affect U238 fast fission, and a varied set of U235 thermal cross sections, are also examined.

In addition, criticality of the uniform lattices (TRX-1 and TRX-2) was calculated by the RCP01 Monte Carlo program, with an explicit three-dimensional full-core representation. Central-core reaction rates and integral parameters were also calculated. For TRX-1, the calculation was run out to obtain the gross spatial variation of integral parameters.

Finally, studies of two small systematic errors connected with measurement of ρ^{28} are described in the appendices.

II. CALCULATIONAL METHODS

ENDF/B cross sections were multigroup processed with ETOMX and ETOTX, which are Bettis versions of ETOG (Ref. 5) and ETOT (Ref. 6). P_3 thermal scattering kernels for hydrogen bound in H_2O were processed with FLAN2, the Bettis version of FLANGEII (Ref. 7), from ENDF/B $S(\alpha,\beta)$ files based on the Haywood kernel.

The MUFT 54 group structure was used from 0.625 eV - 10 MeV with multigroup cross sections averaged over a detailed spectrum for a fission source in H_2O. Thermal data were described at 25 energies. Inelastic scattering was described by a multigroup transfer matrix which included multiplication due to the n,2n reaction. Elastic scattering was described in P_3 angular approximation by multigroup.

In addition to the multigroup data, for each resonance absorber RCP01 described Doppler broadened resonance profiles at approximately 25000 energies over the ENDF/B-prescribed resonance range. S-wave resonances were treated explicitly except that only one set of unresolved parameters was allowed over the unresolved range. For U238 the difference from the ENDF/B-prescribed multiple sets was made up in smooth (i.e., multigroup) absorption cross sections. Resolved P-wave resonances for U238 were smoothed as were U235 unresolved resonances. These are both good approximations in these lattices.

The RCP01 cell calculations treated the geometry explicitly in two dimensions. They were run as eigenvalue problems, which accounted for the very slight fission source shape in the fuel rod. A Σ_A/Σ_T estimator and neutron weights were used epithermally. Thermally, a binomial estimator was used in the fuel and a terminating Σ_A/Σ_T estimator in the clad and moderator.

In the "RCP01/P7MG" method, leakage corrections were obtained by means of a multigroup calculation, with cross sections closely matching those of the Monte Carlo. For the uniform lattices, the epithermal calculation was done with MUFT7, which treated a homogenized, simply-buckled lattice in the B1 approximation using the measured total B^2. In the ENDF/B-IV analyses, an "L-factor" was used to force the U238 capture in the zero-buckling MUFT7 calculation to match that of RCP01 above 0.625 eV. A single L-factor was applied to U235 absorption (fission plus capture) in a similar manner.

Thermally, a DP1 calculation was done in 25 energy groups. Thermal cell-flux-weighting factors were derived from U235 fission thermal disadvantage factors obtained in the RCP01 cell calculations. Cell-flux-weighting factors for a single fast group (10 MeV - 821 keV) were derived similarly from the U238 fission fast advantage factors of the RCP01 cell. (For this purpose traces of U235 and U238 were included in the water of the RCP01 cell). The cell-average-flux level was used for the clad. Although relatively unsophisticated, the MUFT flux weighting schemes appear to be quite adequate in this application, when properly applied.

Leakage corrections for the two-region lattices were obtained with P7MG, which performed radial, one-dimensional, 54-multigroup calculations in cylinder geometry for a homogenized lattice. The calculations were P3 epi-thermally and double-P1 thermally. There was one thermal group, with constants condensed from a 25-group calculation for each homogenized core region.

In all cases, leakage correction factors for the RCP01-calculated fast and thermal reaction rates were obtained as the ratio of reaction rate in the leaking, homogenized lattice to that in the homogenized lattice with zero

buckling. Reaction rates were normalized to one neutron born of all fission.

The cross section sensitivity studies with P7MG employed a new resonance treatment (developed by E. Schmidt and L. Eisenhart) based on integral transport theory, with two-dimensional explicit geometry (including clad and void) for the rod-lattice cell. This model, which supersedes the "L-factor" method, used the same detailed cross section profile as RCP01. Within the energy range .625 eV - 5530 eV (to which the new method is limited at present) resonance capture rates were found to agree with RCP01 to better than 1% for these lattices. This method will be used in future calculations.

Present results differ somewhat from those reported previously in the CSEWG thermal data comparison (ENDF-230). This reflects the fact that the calculations have been completely redone with several corrections and improvements, and with much better Monte Carlo statistics. Specifically:

(1) Eigenvalue RCP01 calculations have been run for the cell, whereas a spatially-flat, fixed source was used previously. This has a slight effect on rates, but it is barely above statistics.

(2) Cell calculations were run out to at least 225000 histories. Previous cell calculations had 50000 histories.

(3) P7MG flux weighting factors were corrected. The factors previously used caused eigenvalues to be ~1% high, due to insufficient leakage, but this had negligible effect on integral parameters.

In the full core RCP01 eigenvalue calculations, the entire lattice was represented explicitly in three dimensions. These calculations are described in Section V.

III. PARAMETER RESULTS OBTAINED WITH ENDF/B-IV DATA

Table 1 shows calculated lattice parameters obtained by the RCP01/P7MG method with ENDF/B-IV data. Also shown are experimental parameter values incorporating a number of systematic corrections evaluated by Sher and Fiarman (Ref. 8). For δ^{28} and ρ^{28} these corrections improve somewhat the consistency of calculation/experiment ratios among the four lattices.

Table 2 shows the calculation/experiment ratios for ENDF/B-IV in comparison with similar results for earlier versions, and Table 3 compares calculated cell reaction rates for Version IV and Version III. The following points are noteworthy:

1. U238 epithermal capture is down 3-4% from Version III, with a corresponding reduction of ρ^{28}, which is now about 5% high relative to experiment.
2. U238 fission is 6-9% above Version III depending on lattice pitch. This is due to the harder fission spectrum and reduced U238 inelastic scattering of Version IV.
3. U235 epithermal fission is down 2% from Version III; thermal fission is up 1-2%. δ^{25} shows a clear dependence on lattice pitch, ranging from 2% low at $V_w/V_u = 8.11$ to 4% high at $V_w/V_u = 1.0$.
4. Total U238 capture is down ~2% from Version III; total U235 fission is up ~1%. CR* is much improved.

Tables 4 and 5 list the calculated major reaction rates for the cell with leakage, and without ($B^2 = 0$).

Table 1

TRX LATTICE PARAMETERS, MEASURED AND CALCULATED WITH ENDF/B-IV DATA

	TRX-3 V_w/V_v = 1.00		TRX-1 V_w/V_u = 2.35		TRX-2 V_w/V_u = 4.02		TRX-4 V_w/V_u = 8.11	
	Exp.	Calc.	Exp.	Calc.	Exp.	Calc.	Exp.	Calc.
ρ^{28}(epi/thermal U238 capture)	3.03 ±.05	3.18 ±.01	1.320 ±.021	1.396 ±.004	.837 ±.016	.867 ±.004	.481 ±.011	.507 ±.003
δ^{25}(epi/thermal U235 fission)	.231 ±.003	.241 ±.001	.0987 ±.0010	.1009 ±.0004	.0614 ±.0008	.0614 ±.0003	.0358 ±.0005	.0352 ±.0002
δ^{28}(U238 fission/ U235 fission)	.167 ±.008	.179 ±.001	.0946 ±.0041	.0964 ±.0003	.0693 ±.0035	.0686 ±.0003	.0482 ±.0020	.0483 ±.0002
CR*(U238 capture/ U235 fission)	1.255 ±.011	1.282 ±.002	.797 ±.008	.809 ±.001	.647 ±.006	.648 ±.001	.531 ±.004	.533 ±.001
λ	1.000	.9899 ±.0012	1.000	.9837 ±.0010	1.000	.9894 ±.0013	1.000	.9880 ±.0016

Table 2

SUMMARY OF PARAMETER RESULTS (ENDF/B-II, III, IV)

Parameter	ENDF/B Version	Calculation/Experiment TRX-3	TRX-1	TRX-2	TRX-4
ρ^{28}	IV	1.050 ± .018	1.058 ± .017	1.036 ± .020	1.054 ± .025
	III	1.088	1.077	1.074	1.082
	II	1.082	1.079	1.071	1.070
δ^{25}	IV	1.043 ± .014	1.022 ± .011	1.000 ± .014	.983 ± .015
	III	1.088	1.045	1.057 (?)	1.003
	II	1.057	1.034	1.023	.989
δ^{28}	IV	1.072 ± .051	1.019 ± .044	.990 ± .050	1.002 ± .041
	III	.983	.944	.943	.946
	II	.934	.904	.894	.920
CR*	IV	1.022 ± .009	1.015 ± .010	1.002 ± .010	1.004 ± .008
	III	1.058	1.040	1.031	1.028
	II	1.059	1.043	1.031	1.026

Table 3

COMPARISON OF ENDF/B-IV AND ENDF/B-III REACTION RATES (B^2=0 CELL)

		Version IV/Version III			
		TRX-3	TRX-1	TRX-2	TRX-4
Epi-thermal	U238 Fission	1.089	1.085	1.060	1.060
	Capture	.971	.972	.960	.959
	U235 Fission	.983	.985	.956(?)	.982
	Q(.625 eV)	1.015	1.005	1.007	1.002
Thermal	U238 Capture	1.005	.994	1.000	.989
	U235 Fission	1.021	1.010	1.015	1.005
	Total U238 Capture	.979	.981	.982	.978
	Total U235 Fission	1.014	1.007	1.012	1.004

Q(.625 eV) is the slowing down rate across 0.625 eV.

Table 4

MAJOR REACTION RATES WITH ENDF/B-IV (B^2=0 CELL)

		TRX-3	TRX-1	TRX-2	TRX-4
Epi-thermal	U238 Fission	.05925 (.32%)	.03933 (.25%)	.02897 (.41%)	.01923 (.47%)
	U238 Capture	.34755 (.19%)	.19904 (.20%)	.12975 (.36%)	.07089 (.51%)
	U235 Fission	.06987 (.23%)	.03897 (.24%)	.02505 (.40%)	.01347 (.56%)
	U235 Capture	.03125 (.33%)	.01753 (.34%)	.01123 (.61%)	.00601 (.80%)
	Q(.625 eV)	.48930 (.13%)	.70005 (.06%)	.79852 (.07%)	.88268 (.05%)
Thermal	U238 Capture	.11279 (.14%)	.14811 (.09%)	.15472 (.13%)	.14047 (.16%)
	U235 Fission	.29638 (.14%)	.39860 (.09%)	.42001 (.12%)	.38385 (.16%)
	U235 Capture	.05206 (.15%)	.06882 (.09%)	.07207 (.13%)	.06552 (.16%)
	K_∞	1.0532 (.10%)	1.1696 (.08%)	1.1586 (.13%)	1.0156 (.16%)

Rates are normalized to one neutron born of all fission. Q(.625 eV) is the slowing down rate across 0.625 eV. Uncertainties are % standard deviations.

ν values are from the MUFTI (or P7MG) calculations.

For TRX 2,3,4 results are based on eight independent calculations of 28,200 histories each, for a total of 225,600 histories. For TRX-1 there were 16 independent calculations totaling 460,000 histories.

Table 5

LEAKAGE CORRECTED MAJOR REACTION RATES (ENDF/B-IV)

		TRX-3	TRX-1	TRX-2	TRX-4
Epi-thermal	U238 Fission	.06055	.03524	.02599	.01868
	ν Fission	.16998	.09918	.07328	.05281
	Capture	.33016	.17217	.11393	.06922
	U235 Fission	.06578	.03351	.02190	.01315
	ν Fission	.16008	.08158	.05334	.03207
	Capture	.02932	.01505	.00981	.00586
	Q(.625 eV)		.59180	.68891	
Thermal	U238 Capture	.10380	.12336	.13141	.13664
	U235 Fission	.27278	.33195	.35669	.37339
	ν Fission	.65979	.80292	.86277	.90316
	Capture	.04791	.05732	.06121	.06374

IV. PARAMETER RESULTS OBTAINED WITH VARIED DATA

A. U238 Capture

At the Seminar on U238 Resonance Capture (Ref. 9) several questions were raised about the ENDF/B U238 resonance representation. Of most likely significance for the prediction of U238 resonance capture in lattices were:

(1) resonance parameter values for the lowest energy U238 resonances,

(2) neglect of contributions to σ_s from resonances outside the resolved resonance range (1 eV - 4000 eV), especially a ladder of negative energy resonances, and

(3) use of the Breit-Wigner single-level formalism, which misrepresents σ_s locally in the resonance wings, particularly in the interference dips where negative σ_s occurs in some instances.

Recent measurements of parameters for the first few resonances of U238 by G. deSaussure, et al. (Ref. 10) and by R. Chrien, et al. (Ref. 11) have yielded Γ_γ values lower than those of ENDF/B-IV and more consistent with the mean Γ_γ = .0235 eV. These data are shown in Table 6.

DeSaussure has recommended (see Ref. 12) a revised ENDF/B-file 3 σ_s for U238 up to 2000 eV to account for the negative energy resonances, revised parameters for the first three resonances, and a revision of the ENDF/B-IV thermal (0-1 eV) σ_s and σ_γ data. These changes are shown in Table 6 and in Figure 1, in comparison with ENDF/B-IV.

The effects of these data variations on U238 resonance capture and other reaction rates in TRX-1 were calculated by two methods:

- RCP01 cell calculations (zero leakage). With the correlated sampling strategy in RCP01, each history has its own random number sequence and remains in step until the varied data are encountered. For the base calculation and for each data variation, ten independent cases were run to obtain an estimate of the uncertainty including the correlation.
- Deterministic MUFT7 calculations for the simply-buckled TRX-1 lattice (B^2 = .0057 cm^{-2}), employing the improved resonance absorption model based on integral transport theory.

The specific cases studied were:

(1) ENDF/B-IV data (base calculation).

(2) Change to deSaussure, et al. measured parameters (Ref. 10) for U238 resonances at 6.67, 20.9, and 36.8 eV (Table 6).

(3) Change to Chrien, et al. measured parameters (Ref. 11) for U238 resonances at 6.67, 20.9, 36.8, 66.15, 80.74, 102.47, and 116.85 eV. (Table 6).

(4) Change to ORNL recommended parameters (Ref. 12) for U238 resonances at 6.67, 20.9 and 36.8 eV. Also, recommended File-3 σ_γ and σ_s (0-1 eV) and File-3 σ_γ (1.0 eV - 2000 eV).

(5) In addition to the changes in (4) also change to ORNL recommended File-3 σ_s, 1.0 eV - 2000 eV. (Accounting for the scattering contribution from the negative energy resonances.) See Figure 1.

(6) In addition to the changes in (5) also change to Reich-Moore multilevel formalism.

Table 6

RESONANCE PARAMETER MODIFICATIONS FOR THE FIRST U238 RESONANCES

E_o(eV)		Resonance Parameters (meV) ENDF/B-IV	Chrien, et al. (Ref. 11)	deSaussure, et al. (Ref. 10)	ORNL Recommended (Ref. 12)
6.67	Γ_n	1.50	1.50	1.482	1.50
	Γ_γ	25.6	21.8	22.96	23.0
20.9	Γ_n	8.80	9.86	10.19	10.0
	Γ_γ	26.8	23.5	22.46	23.0
36.8	Γ_n	31.1	33.3	33.85	33.5
	Γ_γ	26.0	23.6	22.29	23.0
66.15	Γ_n	25.3	25.6		
	Γ_γ	23.5	22.2		
80.74	Γ_n	2.0	2.16		
	Γ_γ	23.5	23.7		
102.47	Γ_n	71.0	68.		
	Γ_γ	26.0	24.3		
116.85	Γ_n	28.3	30.		
	Γ_γ	23.5	23.4		

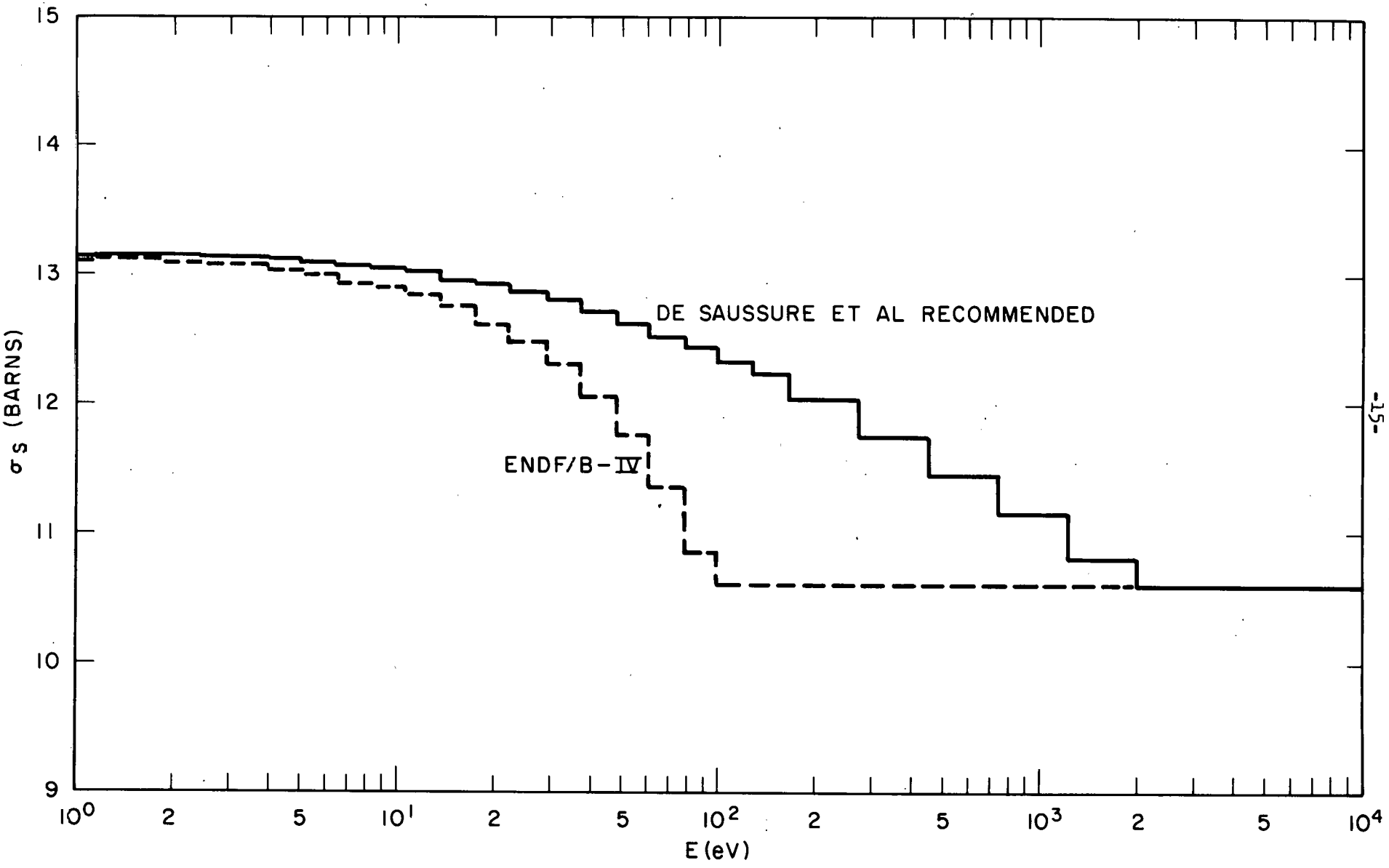

Figure 1 - Comparison of ENDF/B-IV and deSaussure-Recommended File 3 Scattering Cross Sections for U238

The effects of these changes on U238 capture in TRX-1 are shown in Table 7. The several resonance parameter modifications produce a 2-3% reduction of ρ^{28} and resultant small changes of other lattice parameters. Inclusion of scattering from the negative energy resonances has negligible effect.

Use of the Chrien parameters in TRX-2, 3, 4 reduced ρ^{28} by 2.7% relative to ENDF/B-IV. This is the same as the response observed in TRX-1.

Use of the Reich-Moore-formalism, in generating the U238 cross section profiles for RCP01, resulted in a 1.1% reduction of U238 resonance capture. This result must be interpreted with some caution because the procedure uses an entirely different portion of the cross section generating machinery, including kernel Doppler broadening, and produces small changes in the dilute capture resonance integrals. D. R. Finch has studied this effect in detail in connection with CSEWG thermal data testing and observes that reasonable changes of the single level σ_s in the interference dips reduces capture by about 1%. Rothenstein (Ref. 9, p. 241) reports a 0.6% ($\pm$ 0.6%) reduction of U238 capture due to use of a multilevel cross section representation. On the basis of these results, it appears that the effect of the multilevel representation is to reduce U238 capture by approximately 1% in these lattices, but additional studies are required to determine the precise effect of a specific representation.

Several additional data variations were examined, as follows:

(7) Replace the ENDF/B-IV U235 fission spectrum (a Maxwellian, $\bar{E}$ = 1.985 MeV) with a Maxwellian, $\bar{E}$ = 2.00 MeV.

(8) Use a Watt spectrum $\bar{E}$ = 2.00 MeV instead.

Table 7

EFFECT OF DATA VARIATIONS ON U238 CAPTURE RATES AND ρ^{28} IN TRX-1

Case	Varied Data/ENDF/B-IV Data: Epithermal U238 Capture (>0.625 eV) RCP01 (± σ)	MUFT7	Thermal U238 Capture (<0.625 eV) RCP01 (± σ)	MUFT7	ρ^{28} = Epi/Thermal U238 Capture RCP01 (± σ)	MUFT7
1) Base (ENDF/B-IV)	1.000	1.000	1.000	1.000	1.000	1.000
2) Change to deSaussure et al. measured parameters (Ref. 10)	.9830 ± .0018	.9820	1.0047 ± .0006	1.0049	.9784 ± .0019	.9772
3) Change to Chrien et al. measured parameters (Ref. 11)	.9777 ± .0022	.9784	1.0060 ± .0008	1.0059	.9719 ± .0025	.9727
4) Change to ORNL recommended parameters and file 3 data except σ_s (1.0 eV-2 keV)	.9833 ± .0023	.9843	1.0039 ± .0010	1.0042	.9795 ± .0025	.9802
5) Same as (4) plus σ_s(1.0 eV-2 keV)	.9884 ± .0030	.9865	1.0013 ± .0024	1.0041	.9871 ± .0038	.9825
6) Same as (5) plus Reich-Moore multilevel formalism	.9787 ± .0074	.9742	1.0060 ± .0025	1.0074	.9729 ± .0078	.9670

(9) Use a Maxwellian $\bar{E}$ = 2.10 MeV (for sensitivity to $\bar{E}$).

(10) Use B. R. Leonard's Thermal U235 data recommended for ENDF/B-V (Ref. 13) (keep ENDF/B-IV $\bar{\nu}$).

The effects of these changes on lattice parameters for TRX-1 (B^2 = .0057 cm^{-2}) are shown in Table 8. The only significant sensitivity is that of δ^{28} to fission spectrum.

V. FULL CORE MONTE CARLO CALCULATIONS

The RCP01/P7MG method described in Section II has been used for many years to analyze these experiments. It was at first the only suitable method available, and has been considered adequate because, except for eigenvalue, leakage affects the integral parameters only in a secondary way and parameter leakage corrections are modest (usually < 5%). The critical eigenvalues, on the other hand, are directly sensitive to the full-core leakage rates, which are determined by P7MG. In TRX-1 and TRX-2, the leakage is about 15%.

In order to obtain an overall calculation of consistent accuracy, Monte Carlo analyses of the uniform TRX lattices have been done with each core represented explicitly in three dimensions. Figures 2 and 3 show the radial RCP01 representation of the lattices, with each clad rod described explicitly. In each case, the lattice was surrounded by a thick water reflector. The axial description of the cores is shown schematically in Figure 4. The aluminum rod tips and handles, and the lattice plate, were represented approximately. Two intermediate 1/4"-lucite lattice spacer plates, at 1/3 and 2/3 of the full rod height (Ref. 14), have been omitted.

Table 8

EFFECT OF ADDITIONAL DATA VARIATIONS ON PARAMETERS IN TRX-1

Variation	Varied Data/ENDF/B-IV Data				
	ρ^{28}	δ^{25}	δ^{28}	CR*	λ
1) Base (ENDF/B-IV)	1.000	1.000	1.000	1.000	1.0000
7) Change fission spectrum to Maxwellian, $\overline{E}$ = 2.00 MeV	1.000	1.000	1.010	1.000	1.0002
8) Change fission spectrum to Watt, $\overline{E}$ = 2.00 MeV	1.001	1.001	1.019	1.000	.9992
9) Change fission spectrum to Maxwellian, $\overline{E}$ = 2.10 MeV	1.001	1.002	1.186	1.000	1.0016
10) Change to Leonard's (Ref. 13) recommended U235 thermal cross sections (except $\overline{\nu}$)	.998	1.001	1.001	1.002	.9998

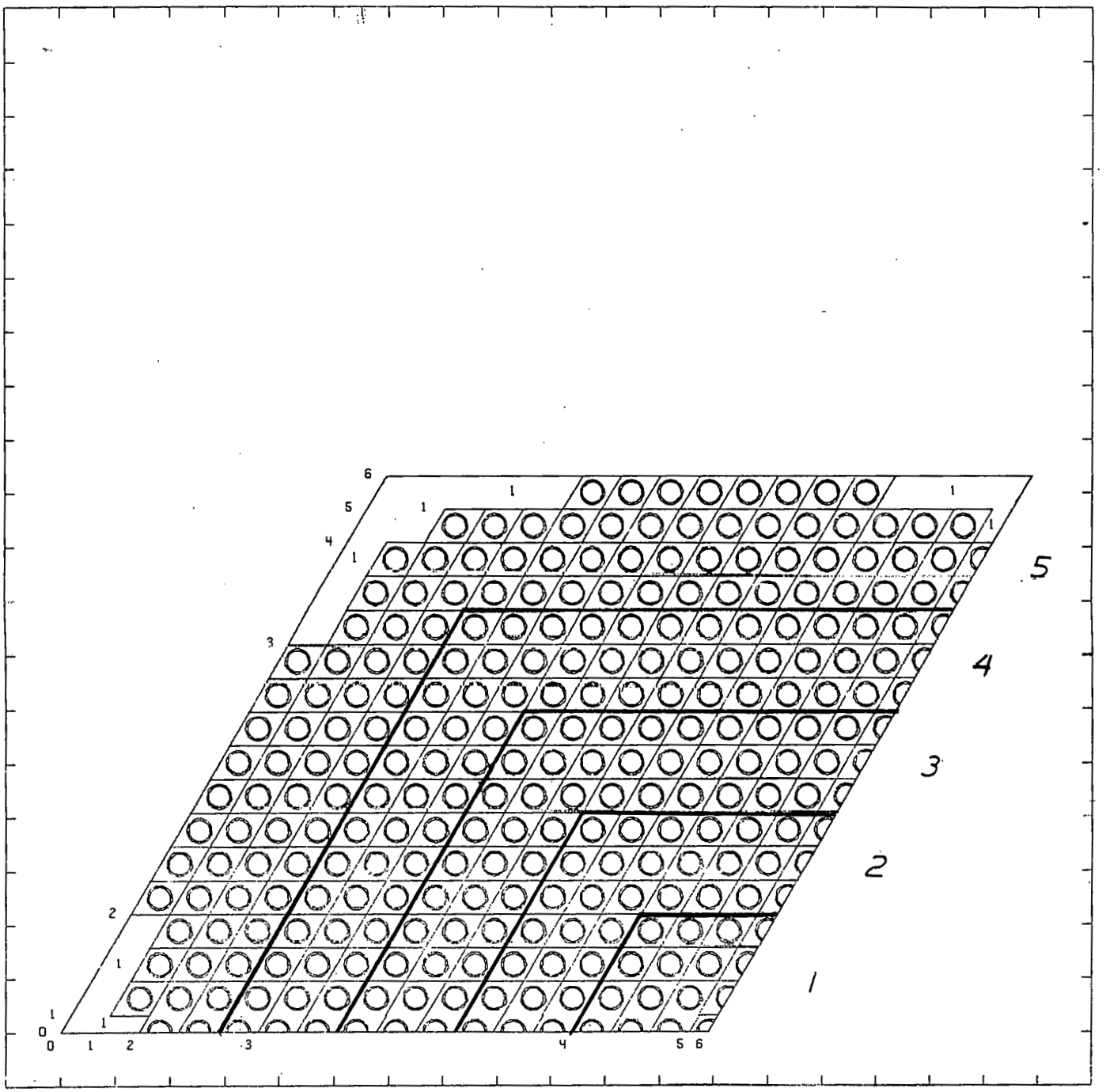

Figure 2 - RCP01 Radial Representation of TRX-1 (1/3 Core)

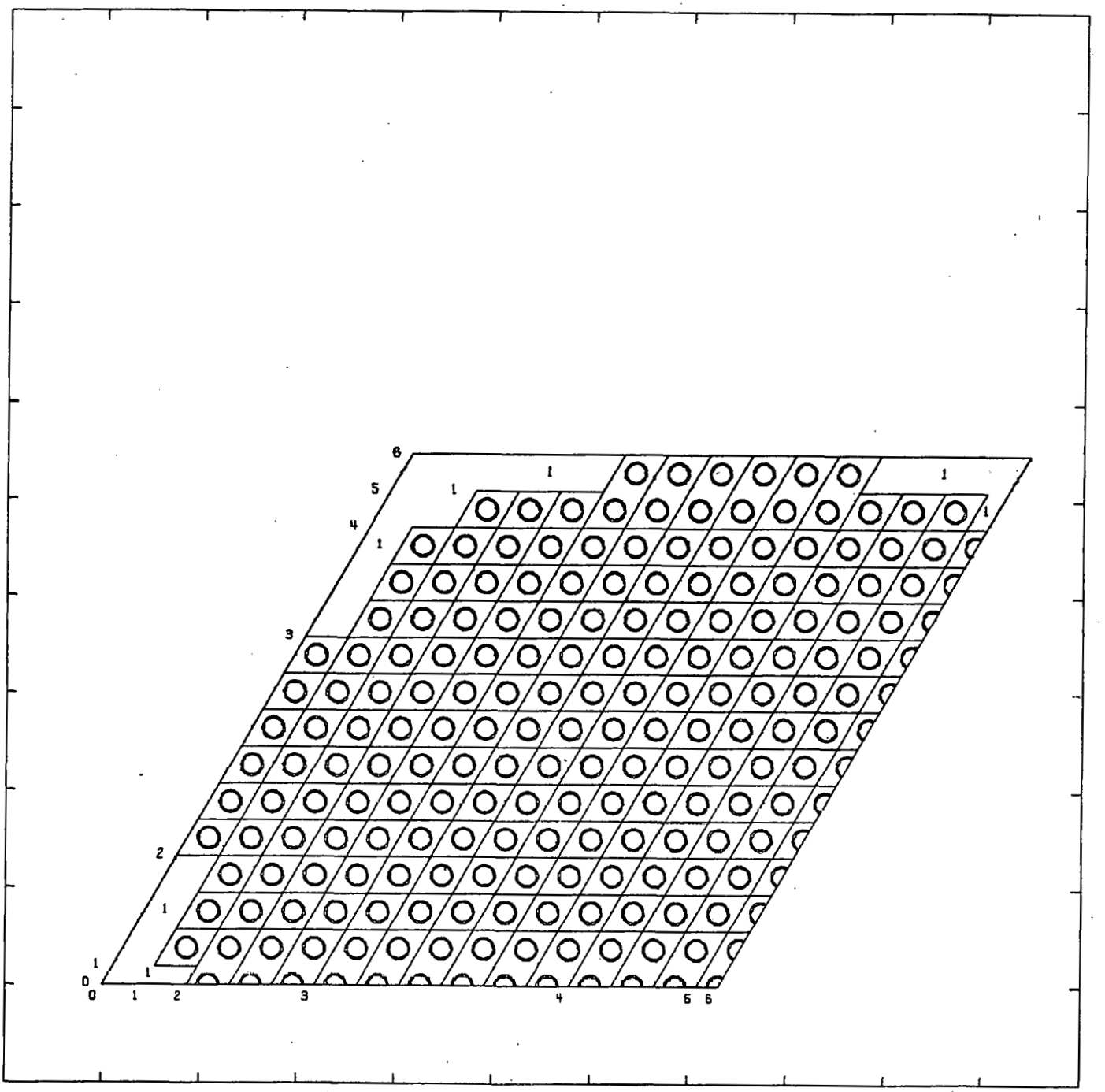

Figure 3 - RCP01 Radial Representation of TRX-2

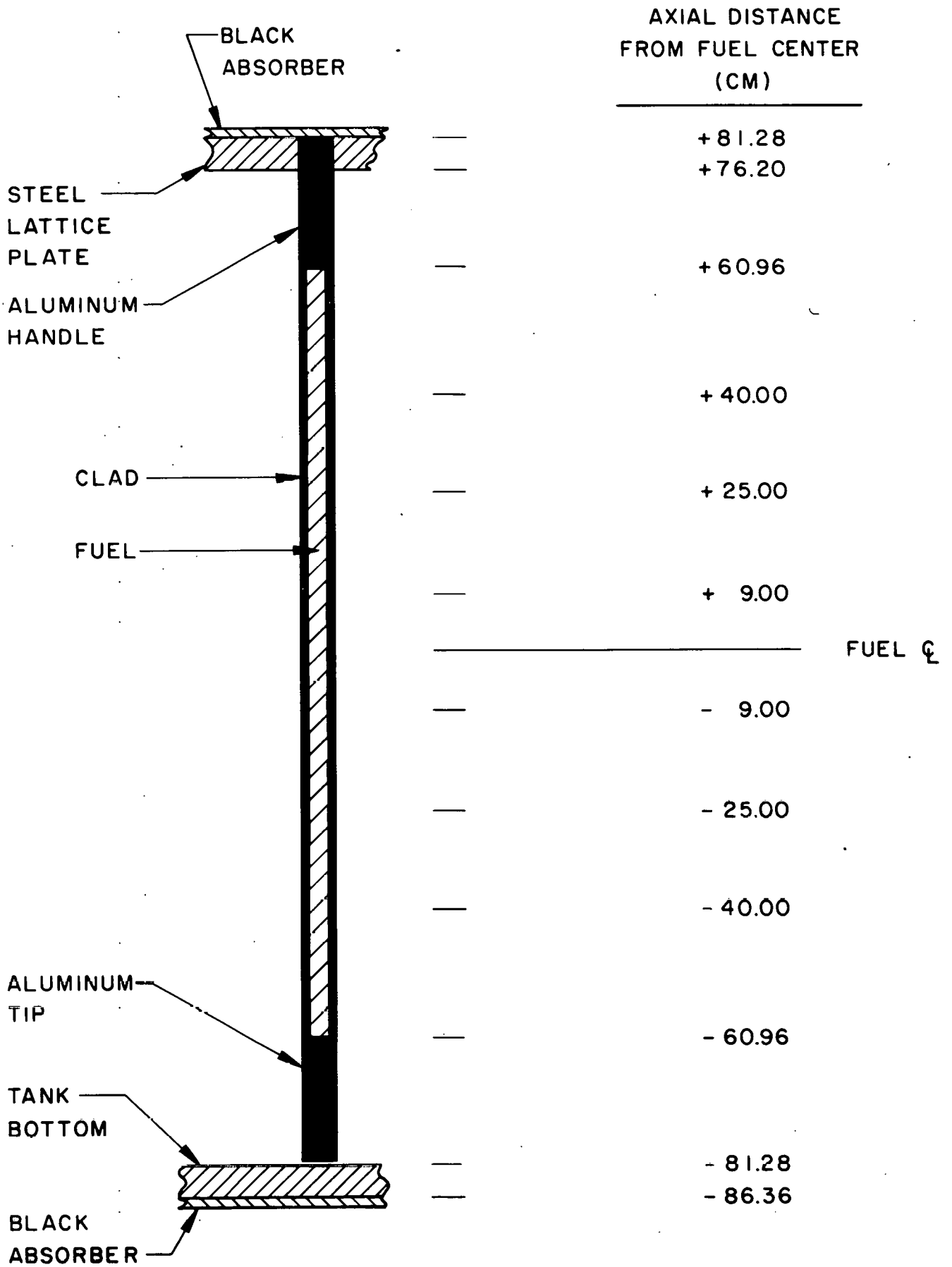

Figure 4 - RCP01 Axial Representation (schematic)

Figures 5 and 6 show radial representations of the two-region lattices. Because these lack a central asymptotic spectrum region large enough to provide good statistics, it is not feasible to obtain integral parameters measured at core center from a full core RCP01 Monte Carlo analysis. Criticality studies of these lattices remain to be completed .

Several independent 100-iteration calculations were run for each core. There were 500 histories in the first iteration; this was increased by 10 histories in each succeeding iteration, for a total of 100,500 histories. The first calculation started with a flat source guess. In subsequent calculations, the initial-source guess was obtained from the final spatially-converged source for the first calculation.

Because of the large central asymptotic regions in TRX-1 and TRX-2, it was possible to obtain good statistics for central core reaction rates and integral parameters. These are directly comparable with the measurements, which were made at (or very near) core center.

For TRX-1, the full core study was made in great detail to determine the spatial variation of reaction rates and integral parameters over gross core regions. Altogether, sixteen independent calculations were run. For editing purposes, the core was divided into five radial regions (labeled hex regions 1-5) comprising hexes 0-3, 4-6, 7-9, 10-12, and 13-16, respectively as shown in Figure 2. Axially, reactions within 20.96 cm of the fuel rod ends were separately edited; in addition, the central portion of each rod was divided into five bands, symmetric about axial center, which were edited in pairs (labeled axial zones I-III) as shown in Figure 4.

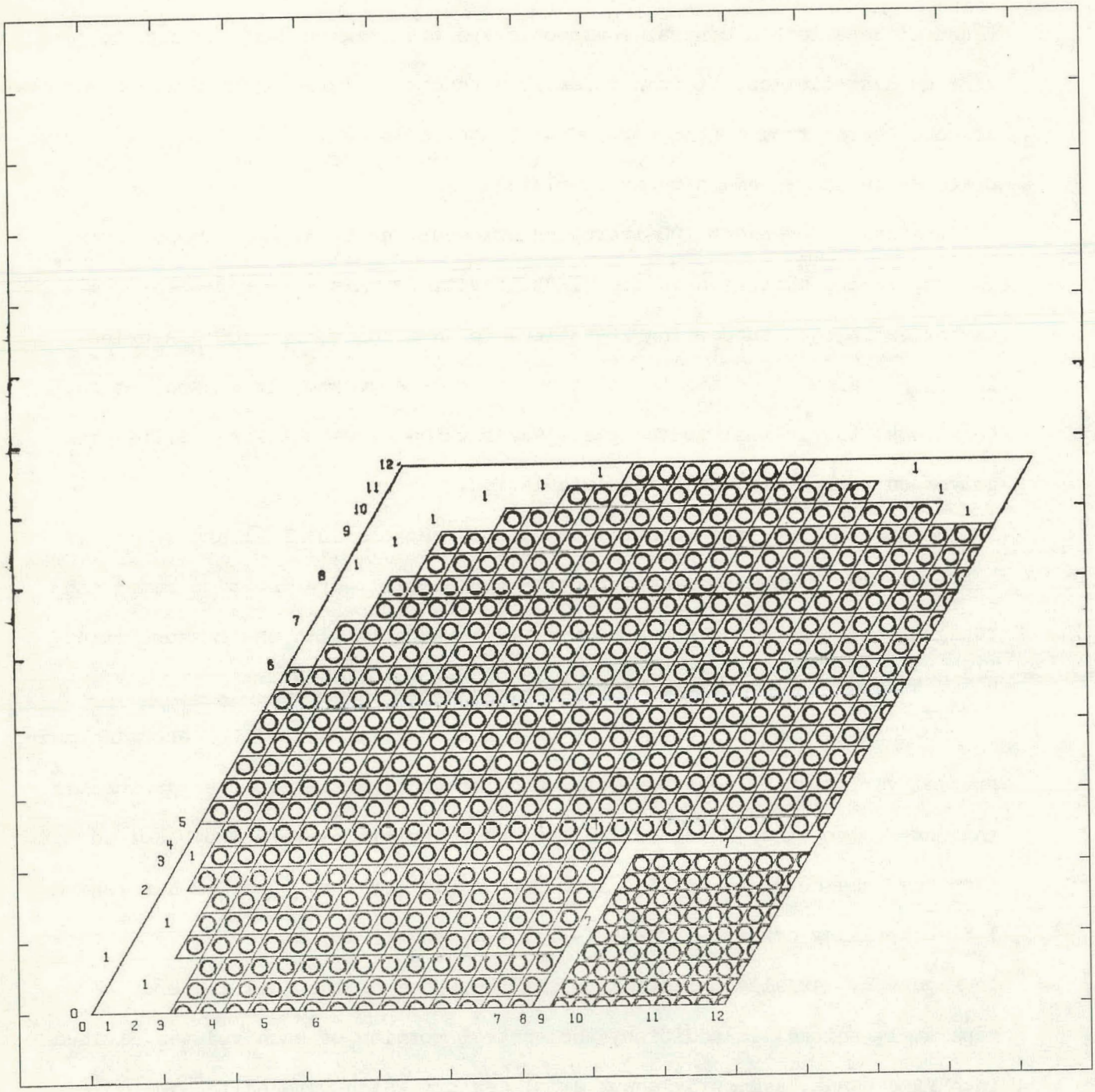

Figure 5 - RCP01 Radial Representation of TRX-3

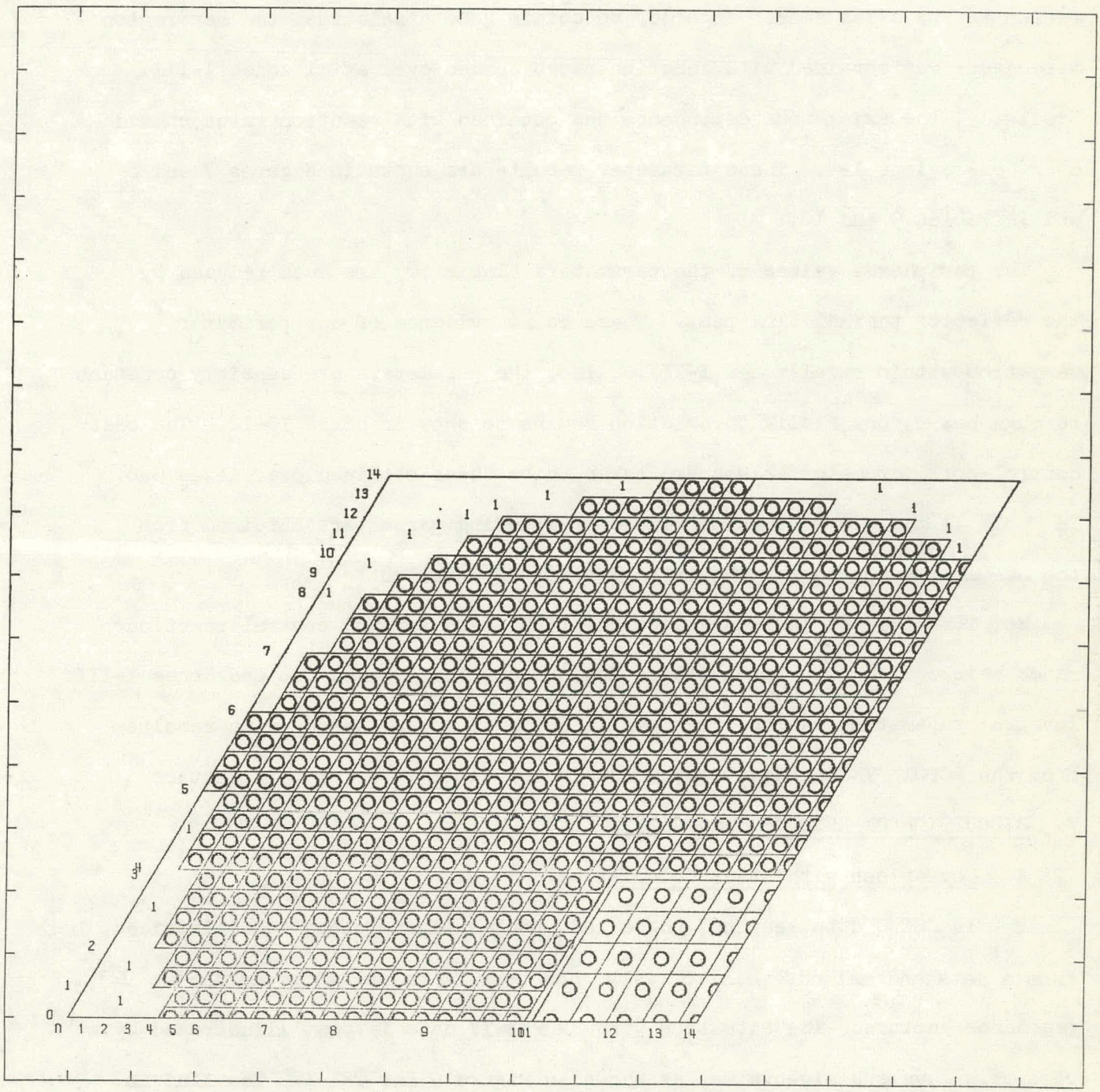

Figure 6 - RCP01 Radial Representation of TRX-4

From the detailed reaction rates, parameter values were calculated by hex region and by axial zone. In order to obtain good statistics, the hex-region dependence was obtained with reaction rates summed over axial zones I-III. Similarly, the axial-zone dependence was obtained with reaction rates summed over hex-regions 1-4. These parameter results are shown in Figures 7 and 8 and in Tables 9 and 10.

The peripheral values of the parameters (Table 10) are much reduced by the reflector thermal flux peak. There is no evidence of any parameter variation within axial zones I-III. Also, the parameters are sensibly constant through hex 9, but a slight variation begins to show in hexes 10-12. The best central-core parameter values are taken to be those obtained over hexes 0-6. In Table 11 these are compared with corresponding parameters obtained from the RCPO1/P7MG method for TRX-1. Agreement is excellent.

For TRX-2, eight independent calculations were run and central reaction rates were edited only for a single region comprising hexes 0-6 and Zones I-III. Integral parameter results are shown in Table 12 in comparison with results from the RCPO1/P7MG method. Agreement is very good also for this lattice

V. DISCUSSION OF RESULTS

A. Comparison with Other Calculations

In CSEWG data testing, the chief problem in analyzing these lattices, both from a data and methods point of view, has been to calculate properly the U238 resonance capture. The situation with ENDF/B-IV data is best illustrated by a plot of ρ^{28} versus eigenvalue, as shown in Figure 9 for TRX-1. The line in this figure is a calculated sensitivity (Ref. 9, p. 27) obtained by varying the unshielded U238 epithermal capture cross section, normalized to the experimental value. The other data points are ENDF/B-IV updatings of the CSEWG data testing

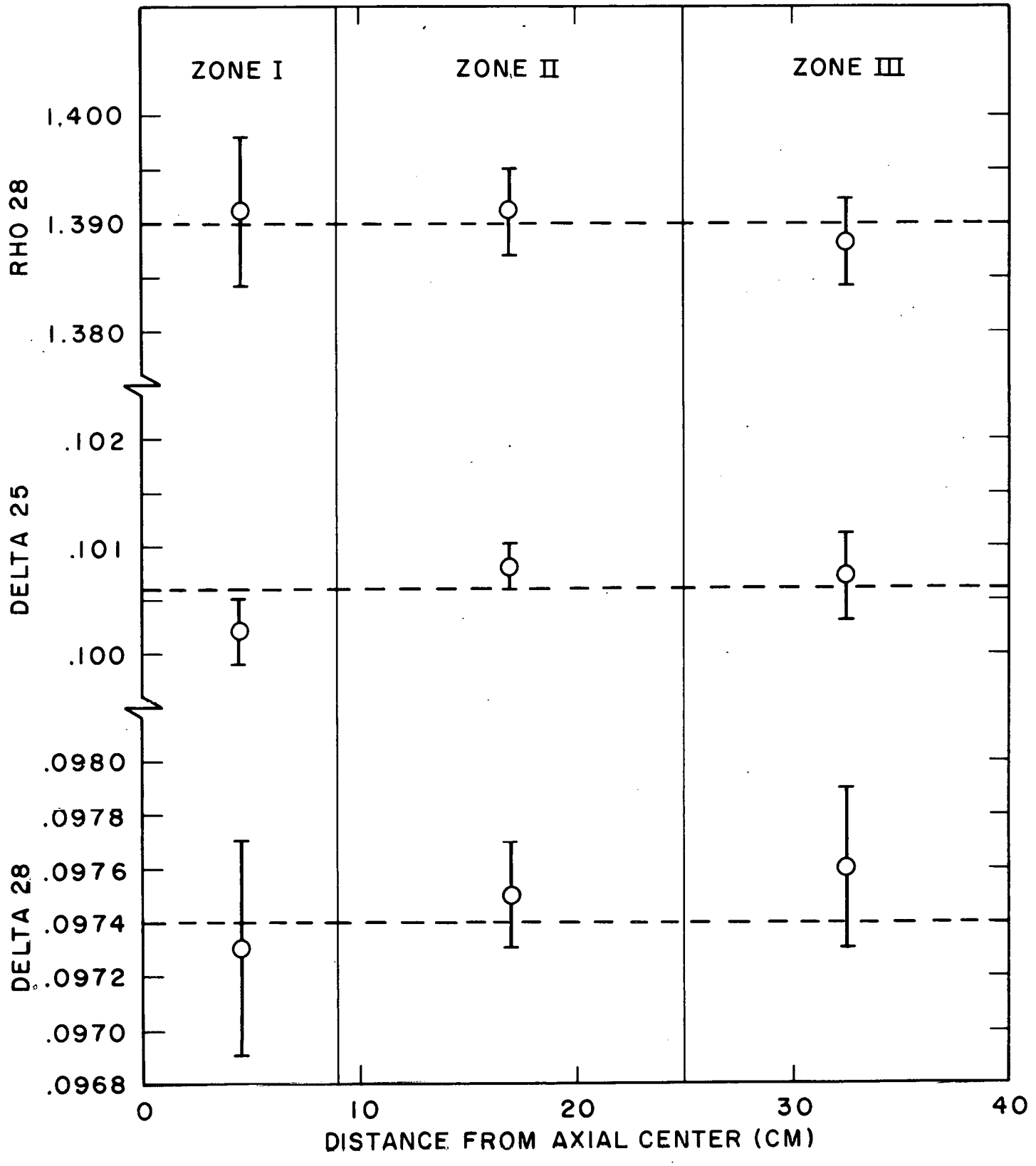

Figure 7 - Calculated Parameter Values by Axial Zone in TRX-1, from Full Core Monte Carlo Analysis

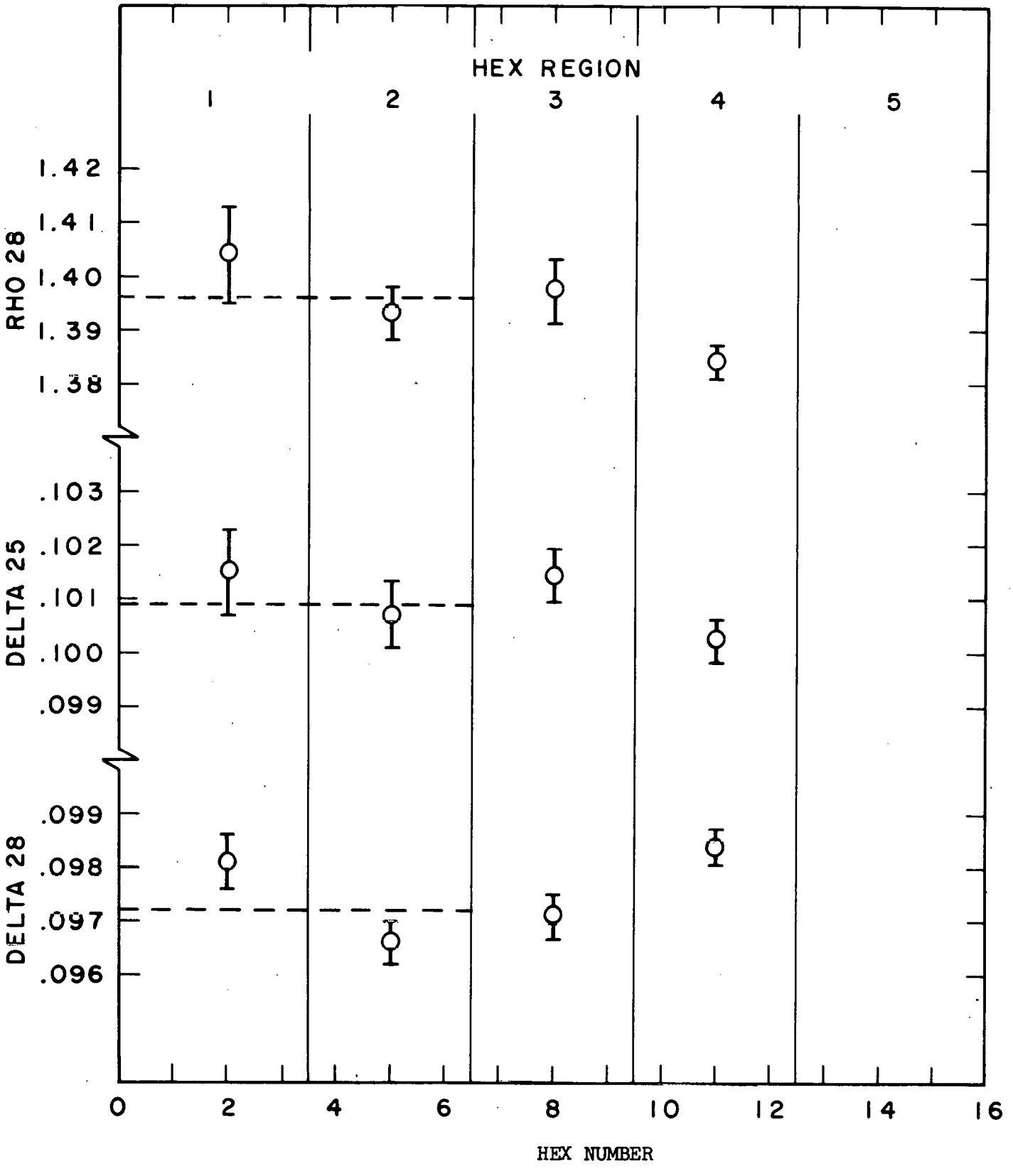

Figure 8 - Calculated Parameter Values by Hex Region in TRX-1, from Full Core Monte Carlo Analysis

Table 9

CALCULATED VALUES OF PARAMETERS BY AXIAL ZONE (TRX-1)

Axial Zone	Distance from Axial Center (cm)	ρ^{28}	δ^{25}	δ^{28}
I	0 - 9.0	1.391 ± .007	.1002 ± .0003	.0973 ± .0004
II	9.0 -25.0	1.391 ± .004	.1008 ± .0002	.0975 ± .0002
III	25.0 -40.0	1.388 ± .004	.1007 ± .0004	.0976 ± .0003
IV	40.0 -60.96 (rod ends)			
I-III	0 -40.0	1.390 ± .002	.1006 ± .0002	.0974 ± .0001

NOTE: Reaction rates are summed over hexes 0-12.

Uncertainties are 1σ obtained from the spread of the individual values.

Table 10

CALCULATED VALUES OF PARAMETERS BY HEX-REGION (TRX-1)

Hex Region	Hexes	ρ^{28}	δ^{25}	δ^{28}	CR*
1	0-3	1.404 ± .009	.1015 ± .0008	.0981 ± .0005	
2	4-6	1.393 ± .005	.1007 ± .0006	.0966 ± .0004	
3	7-9	1.397 ± .006	.1014 ± .0005	.0971 ± .0004	
4	10-12	1.384 ± .003	.1002 ± .0004	.0984 ± .0003	
5	13-16	~1.16	~.084	~.087	
1&2	0-6	1.396 ± .004	.1009 ± .0005	.0972 ± .0003	.809 ± .001

NOTE: For hexes 0-12, reactions are summed over the central portions of the rods (Zones I-III). The peripheral hex results (hexes 13-16) include also reactions within 20.96 cm of each end of all rods in the lattice.

Uncertainties are 1σ obtained from the spread of the individual values.

Table 11

COMPARISON OF TRX-1 INTEGRAL PARAMETERS OBTAINED BY THE FULL-CORE-RCP01 and RCP01/P7MG METHODS

Integral Parameter	Zero-Leakage Cell (RCP01)	Center of Actual Core	
		RCP01/P7MG	Direct RCP01
ρ^{28}	1.334 ± .004	1.396 ± .004	1.396 ± .004
δ^{25}	.0970 ± .0004	.1009 ± .0004	.1009 ± .0005
δ^{28}	.0896 ± .0003	.0964 ± .0003	.0972 ± .0003
CR*	.793 ± .001	.809 ± .001	.809 ± .001
λ	1.1696 ± .0009	.9837 ± .0008	.9839 ± .0006

Table 12

COMPARISON OF TRX-2 INTEGRAL PARAMETERS OBTAINED BY THE FULL-CORE-RCP01 AND RCP01/P7MG METHODS

Integral Parameter	Zero-Leakage Cell (RCP01)	Center of Actual Core	
		RCP01/P7MG	Direct RCP01
ρ^{28}	.839 ± .003	.867 ± .004	.867 ± .005
δ^{25}	.0596 ± .0003	.0614 ± .0003	.0622 ± .0003
δ^{28}	.0651 ± .0003	.0686 ± .0003	.0698 ± .0004
CR*	.639 ± .001	.648 ± .001	.648 ± .002
λ	1.1586 ± .0013	.9894 ± .0013	.9865 ± .0008

results summarized by F. J. McCrossen at the Seminar on U238 Resonance Capture (Ref. 9, p. XIV).

In Figure 9, the strong correlation between eigenvalue and ρ^{28} results suggests that differences in calculated U238 resonance capture are the chief source of the eigenvalue differences. It also lends support to the measured ρ^{28}, inasmuch as a calculation which reproduces this ρ^{28} can be expected to give a correct λ. (The uncertainty of λ due to uncertainties of data other than U238 σ_c is relatively small). Leakage calculations by the different data testers appear to be consistent, since individual leakage errors would tend to disperse λ while having little effect on ρ^{28}.

The U238 capture situation is similar for TRX-2, as shown in Figure 10. The ORNL analysis (Ref. 12) obtains a 0.9% standard deviation of ρ^{28} from differential data uncertainties. Once again the calculated ρ^{28} and eigenvalue results are highly correlated. For this lattice, they fall about 0.5% below the calculated sensitivity line, which suggests that criticality is best predicted at a ρ^{28} slightly below the measured value. (Note that the calculation/experiment ratio is only 1.036 for this lattice, while for the others it is closer to 1.05, as shown in Table 2, so that the measured ρ^{28} may be slightly high).

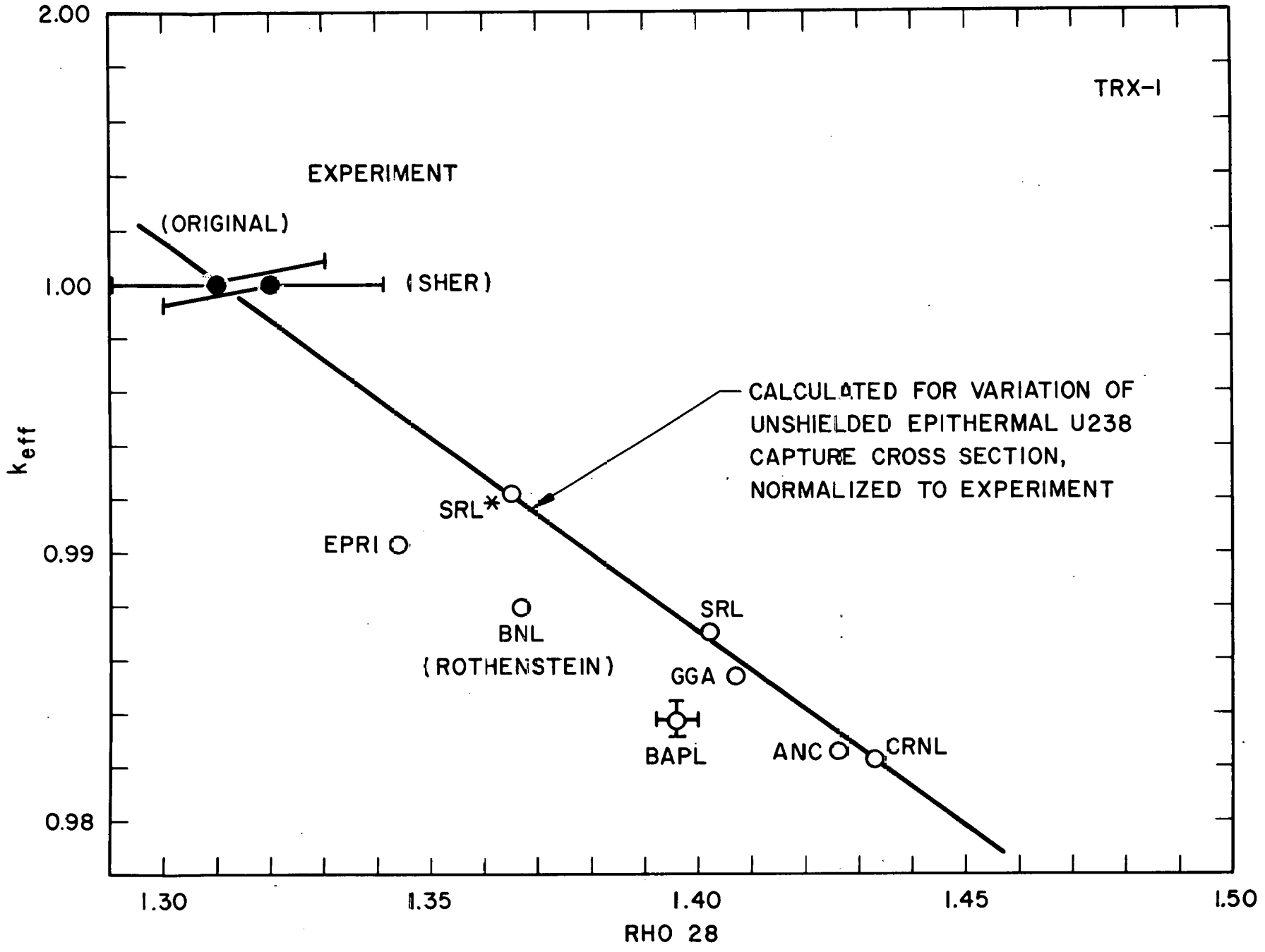

Figure 9 - K_{eff} Versus Rho 28 for TRX-1

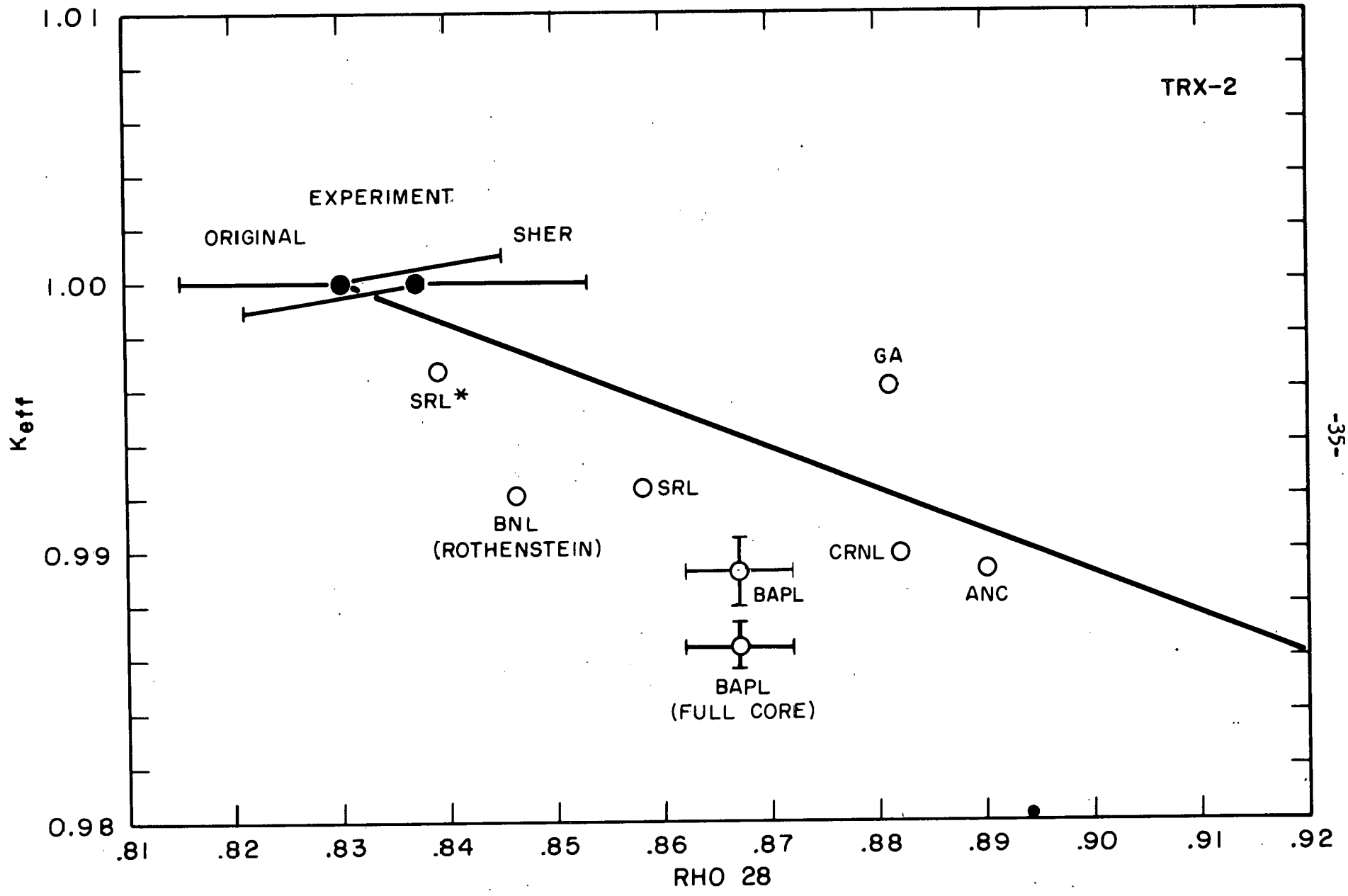

Figure 10 - K_{eff} Versus Rho 28 for TRX-2

Of course, λ is sensitive to other data which do not much affect ρ^{28}. This should not be too important, however, because the ORNL study of TRX-2 obtains a $\pm$ 0.4% uncertainty of λ from all differential data uncertainties, and the contribution from data not affecting ρ^{28} should be less than this.

The RCP01 two-group cell reaction rates for TRX1-4 were compared with results of W. Rothenstein who used the REPC Monte Carlo program for the resonance range, the HAMMER program otherwise (Ref. 16). There was good agreement, except for the following (all 0.625 eV - 10 MeV, RCP01/Ref. 16):

- U238 capture showed a pitch dependent difference ranging from 1-3% for V_W/V_U from 1.0 to 8.11 (see also Figures 9 and 10).
- U238 fission showed a similar pitch dependent difference ranging from 0-4%.
- U235 capture was uniformly high by 3%.

Two additional calculational comparisons should be mentioned:

- Reaction rates obtained with the RECAP-12 Monte Carlo program by Levitt and Rose showed very good agreement with RCP01 in the cell for TRX1 and TRX2. Differences of several percent in the central full-core Monte Carlo parameter results appear to be due to statistics.
- Integral parameter results and two-group reaction rates for TRX-2 calculated by E. T. Tomlinson et al. (Ref. 12) with the ANISN and KENO programs show good agreement with RCP01/P7MG. The Ref. 12 eigenvalue is more than 1% above RCP01/P7MG, apparently due to an underprediction of leakage which has negligible effect on the other parameters.

B. Comparison with Experiment

With ENDF/B-IV, the RCPO1/P7MG values of ρ^{28} are 3.5% - 5.5% above experiment, and a ~2.5% reduction of calculated ρ^{28} can be expected by use of new resonance parameters (see Section IV), which leaves ρ^{28} 1% - 3% above experiment. At this level, many factors can be important and some additional improvement may be obtainable (from a better resonance representation, for example).

The uncertainty of ρ^{28} from differential data is 0.9% (Ref. 12) and an overall uncertainty of 2% is assigned to the integral measurements. Differences among the calculational methods, even among the presumed best methods, are 2-3% and now constitute the most important area of uncertainty.

It is considered that a satisfactory situation will be attained when the presumed good methods agree on ρ^{28} to 1% and with integral experiment to 2%.

The RCPO1/P7MG-calculated values for other integral parameters are in reasonably good agreement with experiment (Tables 1 and 2). There is a clear lattice pitch dependence of the calculation/experiment ratios for δ^{25}, and this is somewhat worse than was apparent before application of the Sher-Fiarman corrections. In all these lattices, a 10 b reduction of the U235 fission resonance integral produces ~3.7% reduction of δ^{25} (Ref. 9, p. 27). The U235 resonance integral sensitivity of δ^{25} shows no significant lattice pitch dependence, however. The ENDF/B-IV U235 fission resonance integral is 284 b above 0.5 eV, somewhat high relative to the best integral value, which is more nearly 275 $\pm$ 5 b (Ref. 18). Thus an improvement of the ENDF/B-IV fission integral would lower δ^{25} by about 3% in all these lattices.

δ^{28} shows reasonable agreement in all lattices, allowing for the experimental uncertainties of 4-5%. Calculated δ^{28} is expected to increase

due to data changes in prospect for ENDF/B-V: hardening of the U235 fission spectrum and modification of the U238 inelastic cross section.

VII. SUMMARY AND CONCLUSIONS

The four TRX CSEWG benchmark cores - simple, H_2O-moderated rod lattices of slightly enriched uranium - were analyzed with ENDF/B-IV data. Measured integral parameters were calculated by a full-range RCP01 Monte Carlo analysis of the zero-leakage cell, with small leakage corrections obtained from a homogenized full-core analysis with P7MG. Calculated parameters (ρ^{28}, δ^{25}, δ^{28}, CR* and λ) are significantly improved over previous ENDF/B versions. They are generally consistent with experiment, except that ρ^{28}, the ratio of epithermal/thermal U238 capture, is high by 5% and eigenvalues are correspondingly low.

Recently measured resonance parameters for the first few resonances of U238 reduce calculated ρ^{28} by 2-3%, significantly improving agreement with experiment.

Full-core Monte Carlo criticality analyses of the uniform lattices (with the cores represented explicitly in three dimensions) produced integral parameters in good agreement with the RCP01/P7MG method. This is fortunate because such full-core Monte Carlo calculations are expensive (due to the added spatial variables) and cannot be applied to parameters measured in marginally asymptotic situations.

Strong correlations between calculated ρ^{28} and λ among the results of CSEWG data testers suggest that the outstanding difference among the various calculational methods is the prediction of U238 resonance capture.

Although the uncertainty of ρ^{28} from differential data is about 0.9% and the integral measurements are uncertain to 2%, differences among the better calculational methods are 2-3%.

REFERENCES

1. J. Hardy, Jr., et al, "A Study of Physics Parameters in Several Water-Moderated Lattices of Slightly Enriched and Natural Uranium," WAPD-TM-931, March 1970.
2. Cross Section Evaluation Working Group Benchmark Specifications, ENDF-202, November 1974.
3. "RECAP-2, A Monte Carlo Program for Estimating Epithermal Capture Rates in Rod Arrays," WAPD-TM-427, 1964.
4. H. Bohl, Jr., et al, "P3MG-1, A One-Dimensional Multigroup P-3 Program for the Philco-2000 Computer," WAPD-TM-272, 1963.
5. D. E. Kusner, S. Kellman, and R. A. Dannels, "ETOG-1, A Fortran IV Program to Process Data from the ENDF/B File to the MUFT, GAM and ANISN Formats," WCAP-3845-1 (ENDF 114), December 1969.
6. C. L. Beard and R. A. Dannels, "ETØT, A Fortran IV Program to Process Data from the ENDF/B File to Thermal Library Format," WCAP-7363, March 1971.
7. H. C. Honeck and D. R. Finch, "FLANGEII (Version 71-1) A Code to Process Thermal Neutron Data from an ENDF/B Tape," DP-1278, October 1971.

REFERENCES (Cont'd)

8. R. Sher and S. Fiarman, "Studies of Thermal Reactor Benchmark Data Interpretation: Experimental Corrections," EPRI NP-209, October 1976.

9. S. Pearlstein (Editor), "Seminar on ^{238}U Resonance Capture," ENDF-217, March 1975.

10. D. K. Olsen, et al., "Resonance Parameters of the 6.67-, 20.9-, and 36.8-eV Levels in ^{238}U, Trans. ANS 23, p. 496, June 1976.

11. H. I. Liou and R. E. Chrien, "Epithermal Neutron Capture in ^{238}U," Nuclear Science Eng. 62, 463 (1977).

12. E. T. Tomlinson, G. deSaussure, and C. R. Weisbin, "Sensitivity Analysis of TRX-2 Lattice Parameters with Emphasis on Epithermal ^{238}U Capture," Trans. ANS 26, 601 (1977).

13. B. R. Leonard, Jr., D. A. Kottwitz, and J. K. Thompson, "Evaluation of the Neutron Cross Sections of ^{235}U in the Thermal Energy Region," EPRI NP-167, Electric Power Research Institute, February 1976.

14. J. R. Brown, et al., "Kinetic and Buckling Measurements on Lattices of Slightly Enriched Uranium and UO_2 Rods in Light Water," WAPD-176, Bettis Atomic Power Laboratory, January 1958.

15. J. J. Ullo and J. Hardy, Jr., "Analysis of Homogeneous U233 and U235 Critical Assemblies with ENDF/B-IV Data," WAPD-TM-1299, October 1977.

16. W. Rothenstein, "Thermal Reactor Lattice Analysis Using ENDF/B-IV Data with Monte Carlo Resonance Reaction Rates," Nuclear Science Eng. 59, 337 (1976).

REFERENCES (Cont'd)

18. S. F. Mughabghab and D. I. Garber, "Neutron Cross Sections," BNL-325, Third Edition, June 1973.

19. E. M. Gelbard, H. B. Ondis, and J. Spanier, "MARC, A Multigroup Monte Carlo Program for the Calculation of Capture Probabilities," WAPD-TM-273, Bettis Atomic Power Laboratory, May 1962.

20. E. F. Plechaty and J. R. Terrall, "Photon Cross Sections 1 keV to 100 Mev," UCRL-50400, Vol. VI (1968).

21. G. Smith, et al, Nuclear Sci. Eng. 8, 449(1960).

22. J. Hardy, Jr., et al, "Measurement of the Dancoff Correction," Nuclear Sci. Eng. 12, 301 (1962).

ACKNOWLEDGMENTS

The dedicated efforts of Stella Dokish in running the calculations, and of Sue Carr in typing the manuscript, are gratefully acknowledged. Valuable discussions have been held with W. Rothenstein, C. R. Weisbin, E. T. Tomlinson, L. Levitt, D. Craig, and other CSEWG thermal data testers.

APPENDIX I

Study of Thermal Flux Perturbation Due to the U238 Detector Foil in TRX Measurements of ρ^{28}

The ρ^{28} measurement employed a 5-mil highly-depleted uranium detector foil (5 ppm U235) between two 1-mil depleted uranium shields. This loading was used in both the cadmium ratio method and the thermal subtraction method (Ref. 1). This U238-detector-plus-shield package created in the 1.3% enriched fuel rod a 7-mil-thick window with significantly reduced thermal absorption cross section due to the absence of U235.

The effect of this perturbation on thermal U238 captures in the detector foil was calculated with the adjoint mode of the MARC Monte Carlo program (Ref. 19) for the four TRX lattices. In this calculation, the detector-foil package was represented explicitly in comparison with a vanishingly thin detector. Results for the ratio of foil-activation/unperturbed-activation are shown in Table I-1. Since there is no apparent variation with lattice pitch the value $1.016 \pm .002$ is used for all four lattices.

During the course of the experiments, a measurement was done in the TRX-1 lattice to compare activation of a bare foil (thermal plus epithermal) for 7-mil- and 17-mil-thick packages. The measured ratio was A(17-mil)/A(7-mil) = $1.002 \pm .004$.

Assume that the 17-mil and 7-mil perturbations (calculated in the TRX-2 lattice) can be applied also in TRX-1 and that the epithermal activation is unperturbed. Since the measured value of epithermal-to-thermal activation (ρ^{28})

is 1.31, the MARC results imply a relative perturbation of the total activation, A(17-mil)/A(7-mil) = 1.008 ± .004. This is consistent with the measured ratio.

Table I-1

U238 Thermal Capture Rate in the Detector Foil Relative to That in a Thin Foil

Lattice	7-mil Gap	17-mil Gap
TRX-3	1.020 ± .005	
TRX-1	1.016 ± .002	
TRX-2	1.013 ± .002	1.031 ± .004
TRX-4	1.017 ± .001	
AV.	1.016 ± .002	

Because of the complementary nature of the cadmium ratio and thermal subtraction methods, an excess thermal activation affects the inferred ρ^{28} differently:

	Cadmium Ratio	Thermal Subtraction
Perturbed Thermal Activation (A_{Th})	$\frac{\delta\rho}{\rho} = -\frac{\delta A_{Th}}{A_{Th}}$	$\delta\rho = +\frac{\delta A_{Th}}{A_{Th}}$
Perturbed Epithermal Activation (A_E)	$\frac{\delta\rho}{\rho} = +\frac{\delta A_E}{A_E}$	$\delta\rho = +\frac{\delta A_E}{A_E}$

Note that, since the thermal subtraction method measures only total bare-foil activation, there is no way of distinguishing whether excess activation is thermal or epithermal.

The effect of the 1.6% excess thermal activation on ρ^{28} results is shown in Table I-2.

Table I-2

Effect of Excess Thermal Activation on ρ^{28} Results

Lattice	Original Values (Ref. 1)			Corrected Values			Corrected ÷ Original
	Cd R	Ther. Sub.	AV	Cd R	Ther. Sub.	AV	
TRX-3	.466	--	.466	.473	-	.473	1.015
TRX-1	.823	.836	.830	.835	.821	.828	.998
TRX-2	1.296	1.327	1.311	1.315	1.312	1.314	1.002
TRX-4	3.01	3.02	3.01	3.06	3.01	3.04	1.010

APPENDIX II

Study of Foil Edge Effects in Activation Gamma Counting for TRX Measurements of ρ^{28}

In the TRX ρ^{28} measurements, gamma activity resulting from U238 capture was counted with a NaI detector in a window centered about 100 keV. The 100 keV gamma rays interact significantly in the U238 detector foil, leading to an increase of counting efficiency for those originating near the edge of the foil (see Figure II-1).

Because thermal activation is essentially flat across the foil, while epithermal activation shows an additional "surface" component (from resonance peaks), this edge effect can lead to a difference of gamma ray counting efficiency for thermal and epithermal U238 capture activation. The effect was estimated as follows.

For activation counting, the 5-mil-thick, 0.387-in. diameter foil was placed on-axis, ~0.2-in. above a 1/4-in. thick NaI crystal of 2.0 in. diameter. For this geometry the gamma ray detection efficiency as a function of radius in the foil was calculated with the MARC Monte Carlo program.

The calculation assumed a one-energy, purely absorbing model, with a total interaction coefficient for 100 keV gammas in uranium of 31.76 cm^{-1} (Ref. 20). The relative efficiency results are shown in Table II-1.

The spatial shape of epithermal U238 capture in a fuel rod of TRX-3 (V_W/V_U = 1.0) was taken from Ref. 21 which compares measured and calculated activation shapes. It was assumed that 22.5% of the activations occur between

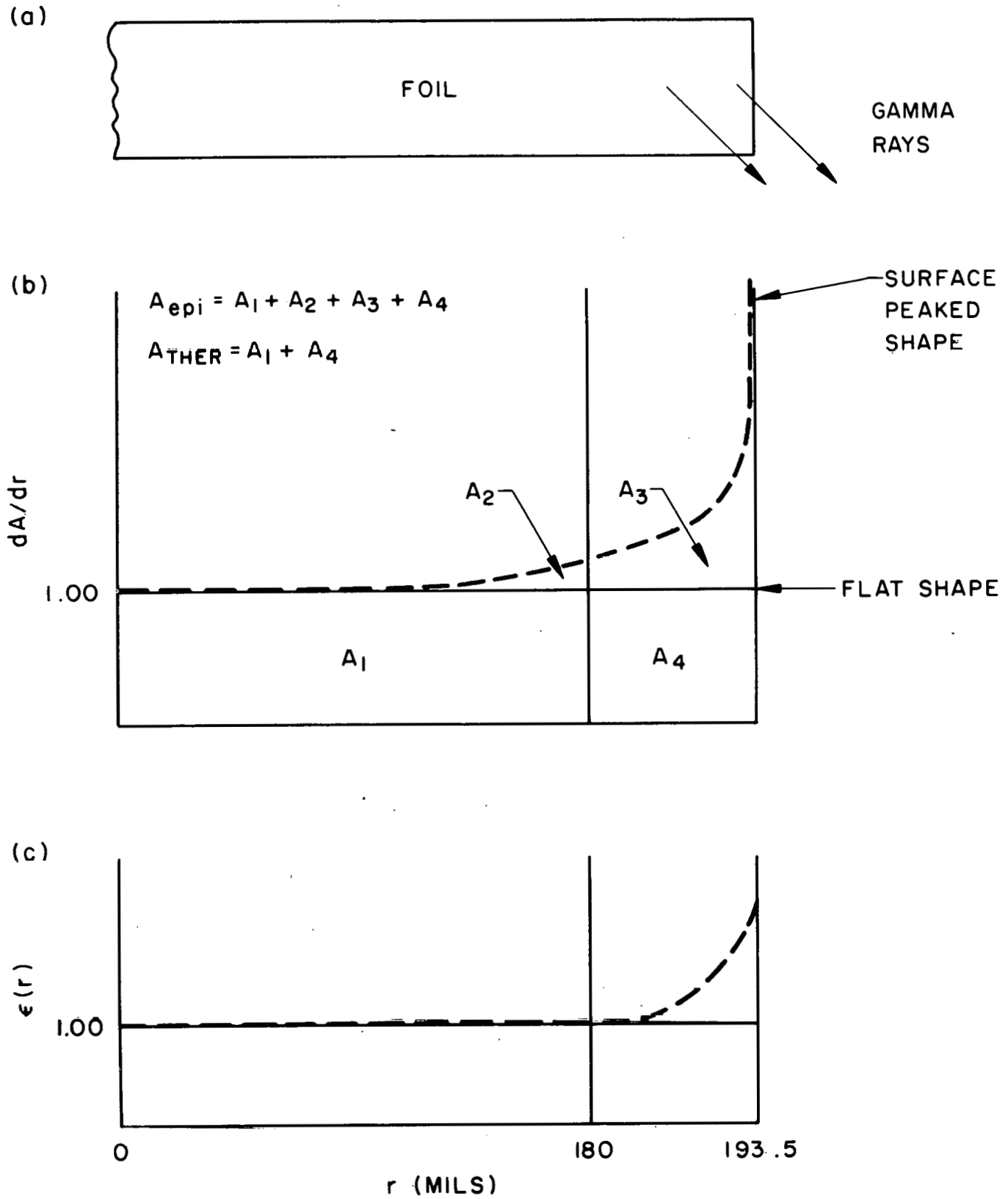

Figure II-1 - Schematic Representations of (a) the edge effect for gamma rays in the U238 detector foil, (b) radial distribution of capture activation in the foil, and (c) radial shape of gamma ray detection efficiency.

radii of 180 - 193.5 mils, and the activation shape in this interval was read from the calculated curve.

The components of the activation are shown schematically in Figure II-1 for a flat and a surface-peaked activation shape. (The A's denote total volume-integrated activation in each component). The relative gamma detection efficiency $\epsilon(r)$ is also shown. It is assumed that the thermal activation shape can be taken as flat.

The effect of folding $A(r)$ and $\epsilon(r)$ can be written (since $\epsilon = 1.0$ except near the edge); $C = \int A(r)\ \epsilon(r)dr$

$$C_{epi} = A_{epi} + A_3(\bar{\epsilon}_3 - 1) + A_4(\bar{\epsilon}_4 - 1)$$

$$C_{Ther} = A_{Ther} + A_4(\bar{\epsilon}_4 - 1)$$

In this case (TRX-3), the calculation yields:

$$\left.\begin{aligned} A_1 &= .70600 \\ A_2 &= .06900 \\ A_3 &= .11512 \\ A_4 &= .10988 \end{aligned}\right\} \quad .225$$

and

$$A_3(\bar{\epsilon}_3 - 1) = .00808$$

$$A_4(\bar{\epsilon}_4 - 1) = .00341.$$

Hence

$$\frac{(C_{epi}/C_{Ther})}{(A_{epi}/A_{Ther})} = \frac{1.23459}{1.22566} = 1.0073$$

Thus, the foil edge effect is estimated to produce a 0.73% excess of ρ^{28} in TRX-3, (the tightest lattice, with $V_W/V_U = 1.0$). At the other extreme, TRX-4 (with $V_W/V_U = 8.1$), the relative surface activation term is 42% higher than in TRX-3 due to the reduced Dancoff interaction (Ref. 22). This should cause ρ^{28} to be high by 1.0%.

Table II-1

Relative Counting Efficiency for 100 keV Gammas as a Function of Radius in Detector Foil

Radius (cm)	Relative Efficiency
.4915	1.1546
.4890	1.0891
.4865	1.0567
.4815	1.0376
.4790	1.0253
.4765	1.0177
.4740	1.0116
.4715	1.0076
.4690	1.0052
.4665	1.0024
.4640	1.0010
.4615	1.0000
↓	↓
0	1.0000

*Statistical uncertainty on each point is 0.25% (σ).

*U.S. GOVERNMENT PRINTING OFFICE: 1978-703-115/198